Criteria Relating Wake Vortex Encounter Hazard to Aircraft Response

Robert I. Sammonds* and Glen W. Stinnett Jr.†
NASA Ames Research Center, Moffett Field, Calif.
and
William E. Larson‡
Federal Aviation Administration, Washington, D. C.

Piloted six-degree-of-freedom motion simulator investigations were conducted at the NASA Ames Research Center to determine criteria relating the hazard posed by a wake vortex encounter to the response of the encountering airplane. These investigations demonstrated that wake vortex encounters can be reproduced realistically on a simulator, established that the maximum bank angle due to the encounter provides the best correlation with the pilot's subjective assessment of the hazard, and determined hazard boundaries in terms of maximum bank angle for two classes of jet transport aircraft.

Nomenclature

IFR	= instrument flight rules
VFR	= visual flight rules
x,y,z	= Cartesian coordinates and distances along these axes
$(\psi,\theta,\phi)_{w/v}$	= Euler angles relating airplane wind axes to the vortex axes
p	= angular velocity about x aircraft axis
$\dot{p}$	= angular acceleration about x aircraft axis
6-DOF	= six-degree-of-freedom motion simulator, designated S.01
FAA	= Federal Aviation Administration
FSAA	= Flight Simulator for Advanced Aircraft, designated S.10

Introduction

INCREASED traffic at major airports in this country has led to a program by the Federal Aviation Administration to develop an "updated third generation" air traffic control system, designed to increase airport capacity and improve safety.[1] The success of this system is dependent upon development of techniques for reducing the current longitudinal separations (4-6 miles) required to avoid the hazard from trailing wake vortices, particularly from large aircraft during approach and landing.[2-8] Research on alleviating the wake vortex hazard is twofold. One aim is to develop a wake vortex avoidance system for the terminal airspace, and the other is to alleviate the hazard by aerodynamic means. In either case, if a wake vortex encounter is likely to occur, it is necessary to distinguish between nonhazardous and potentially hazardous encounters in order to assure safe landings. To accomplish this, it will be necessary to evaluate the hazard of a potential encounter as a function of the aircraft pair, separation distance, and local meteorological conditions. An integral and critical part of such an evaluation are criteria that relate the response of the aircraft (upset magnitude) to the hazard associated with the encounter.

Determination of these criteria, relating the hazard of the encounter to the magnitude of the upset, was the purpose of a joint NASA/FAA research program conducted in the Ames Research Center six-degree-of-freedom piloted motion simulators. These criteria were determined from the subjective assessment by a number of pilots of numerous simulated wake vortex encounters during a landing approach task. No attempt has been made to relate the magnitude of the upset to specific aircraft pairs or separation distances. Such a relationship is outside of the scope of this investigation. The primary objectives of the program were as follows: 1) validate the ability of simulators to produce realistic wake vortex encounters; 2) isolate correlating parameters in the data; 3) determine hazard criteria in terms of aircraft response for two classes of aircraft; and 4) provide data for the development of a pilot model for use in unmanned simulations. The two classes of aircraft of interest were represented by a light, general aviation, twin-jet (Learjet) and a large four-jet transport (Boeing 707/720). The pilot model was developed separately by Systems Technology, Inc. under contract.[9]

Simulation

Description of Simulators

The investigations were conducted using the two NASA Ames Research Center six-degree-of-freedom motion simulators shown in Fig. 1. The motion limits of each of the simulators are given in Table 1. The simulator cabs were equipped with instrumentation for VFR and IFR landing approach tasks (Table 2) as well as throttle, gear, and flap controls to allow abort, clean-up, and go-around (Table 3). The cabs were also equipped with hydraulically actuated control loaders, programmed to give the desired dynamic force-feel characteristics of each aircraft during the landing approach phase of flight.

The pilot in the cab was provided with visual and aural cues, as well as motion cues. The visual cues consisted of a landing approach scene displayed on a T.V. monitor above the instrument panel. The simulator shown in Fig. 1a was equipped with a black-and-white monitor without collimation, whereas the one shown in Fig. 1b had a collimated color presentation. The visual scene in both cases was generated by a computer-driven six-degree-of-freedom T.V. camera, which duplicated the aircraft motion with respect to the landing approach scene. Although the simulator

Presented at the AIAA 3rd Atmospheric Flight Mechanics Conference, Arlington, Texas, June 7-9, 1976 (in bound volume of Conference papers, no paper number); submitted June 24, 1976; revision received April 22, 1977.

Index categories: Navigation, Communication, and Traffic Control; Jets, Wakes, and Viscid-Inviscid Flow Interactions; Safety.

*Research Engineer. Member AIAA.

†Research Pilot.

‡Research Engineer.

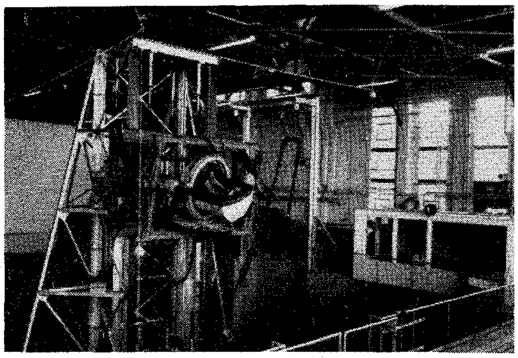

a) Ames six-degree-of-freedom moving base simulator (S.01)

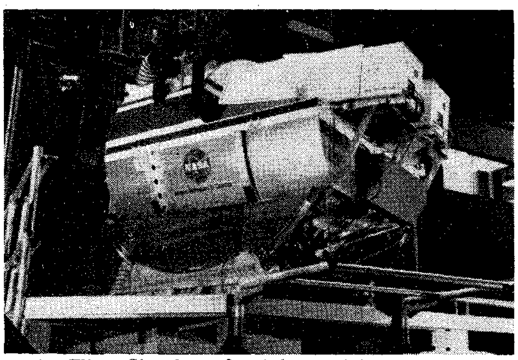

b) Flight Simulator for Advanced Aircraft (S.10)

Fig. 1 Simulators.

motion was restricted by physical limitations, the visual scene was not subject to these same restraints. The aural cues consisted of engine noise modulated by computed engine rpm, and were introduced through stereo speakers located in the cab. The simulator motion systems and the frequency response characteristics of both simulators and visual systems are documented in Refs. 10 and 11.

Modeling

Conventional simulation math models were developed to represent two classes of aircraft having significantly different inertia and response characteristics. These models represented the Gates Learjet Model 23 and the Boeing 707/720, and included approach, go-around, and takeoff configurations. The forces and moments resulting from a vortex encounter were simply superimposed upon those computed for the conventional math model.

The vortex model was defined by a pair of two-dimensional vortices. The parameters that characterized the flowfield in each case were vortex spacing, core diameter, and circulation strength. The tangential velocity from each vortex was calculated from the following equation, and the resultant velocity at a given point was computed in the manner described in Refs. 12 and 13:

$$|V_T| = \frac{\Gamma_0}{2\pi r}\left[1 - e^{-r^2/4\epsilon\tau}\right] \tag{1}$$

where V_T is the tangential velocity; Γ_0 is the vortex strength (a function of the weight, speed, and wingspan of the generating airplane); $\epsilon = 0.0002$, which represents the vortex decay effect; τ is the vortex age; and r is the radial distance from the center of the vortex.

The tangential velocity out to a radius of 35 ft (10.67 m) was determined according to Eq. (1), and then decreased linearly to become 0 at a radius of 70 ft (21.34 m). The objective of this truncation of the flowfield was to make it impossible for the pilot to sense the presence of the vortex at greater distances and preserve the characteristic suddenness of the upsets observed in flight. Three core diameters were selected during the initial phase of the program, but the variation in core diameter was demonstrated to have a negligible effect on the calculated upset. Consequently, one core diameter was used for the majority of the program.

The axes of the two vortices from the generating airplane were assumed to be straight lines, and to be separated by 84 ft (25.6 m) and 150 ft (45.9 m) for the Learjet and 707/720 simulations, respectively. These separation distances are typical of those for the Boeing 727 and 747, respectively, in the landing configuration.

Encounter Geometry

The severity of a vortex upset depends not only on vortex strength, but also on the encounter conditions (i.e., how close the aircraft comes to the vortex core and the angle of the flight path relative to the vortex axis). These encounter conditions were specified in terms of a target point and an entry angle, as shown in Fig. 2. The target point specifies how close the aircraft's initial velocity vector (aircraft C.G.) comes to the vortex core, and the entry angle specifies the attitude of the velocity vector relative to the vortex axis. To ensure that the aircraft's center of gravity would traverse the target point and obtain repeatable encounters, the vortex origin was translated and rotated in such a manner that the aircraft's center of gravity was always heading toward the target point, regardless of aircraft motions. Just prior to reaching the target point, the vortex was frozen in inertial space. The location of the freeze point was selected close enough to the target to ensure penetration, regardless of pilot maneuvering. For the present simulations, the target point was always located at the center

Table 1 Simulator motion limits

Motions generated	Displacement	Acceleration	Velocity
		6-DOF (S.01)	
Roll	±35°	10.0 rad/s²	1.3 rad/s
Pitch	±35°	4.5 rad/s²	1.7 rad/s
Yaw	±35°	3.0 rad/s²	3.0 rad/s
Vertical	±9 ft (±2.7 m)	8.8 ft/s² (2.7 m/s²)	7.5 ft/s (2.3 m/s)
Longitudinal	±9 ft (±2.7 m)	7.5 ft/s² (2.3 m/s²)	9.0 ft/s (2.7 m/s)
Lateral	±9 ft (±2.7 m)	9.2 ft/s² (2.8 m/s²)	8.0 ft/s (2.4 m/s)
		FSAA (S.10)	
Roll	±36°	1.6 rad/s²	0.5 rad/s
Pitch	±18°	1.6 rad/s²	0.5 rad/s
Yaw	±24°	1.6 rad/s²	0.5 rad/s
Vertical	±4 ft (±1.22 m)	12 ft/s² (3.66 m/s²)	7 ft/s (2.13 m/s)
Longitudinal	±3 ft (±0.91 m)	8 ft/s² (2.44 m/s²)	5 ft/s (1.52 m/s)
Lateral	±40 ft (±12.19 m)	10 ft/s² (3.05 m/s²)	16 ft/s (4.88 m/s)

Table 2 Cockpit instrumentation

Instrument
Indicated angle of attack
Indicated airspeed, kt
Turn/bank
Attitude deviation indicator
Horizontal situation indicator (glideslope on right and localizer on bottom)
Control surface status (trim)
Altimeter
Instantaneous vertical speed indicator
Normal acceleration, *g* units
Clock
Engine rpm
Flap deflection
Gear status lights: UP, DOWN

of the vortex core. A more detailed explanation of the encounter geometry and the technique for obtaining repeated encounters is given in Ref. 12.

Vortex-Aircraft Interaction Model

The forces and moments due to the presence of the vortex flowfield were calculated by strip theory, using the methods shown in Refs. 12 and 13. In brief, this procedure divides the wing, horizontal tail, and vertical tail into N number of chordwise strips. (For this case, the wing was divided into 20 strips per semispan, whereas the horizontal and vertical tails were divided into 6 strips per panel for each aircraft.) The local velocity, angles of attack and sideslip, and forces and moments (referred to the airplane center of gravity) due to the vortex were calculated for each strip. These incremental forces and moments were summed and combined with estimated fuselage contributions to give the net forces and moments on the airplane due to the vortex.

Turbulence Model

Turbulence was introduced to obtain the pilot response to a known disturbance for the development of pilot describing functions.[9] The turbulence model used is described in detail in Ref. 12.

Test Program

Task

The test program was limited to vortex encounters during landing approach. The piloting task was to fly either an IFR or VFR approach on a 3° glide-slope, starting with the aircraft trimmed on glide-slope and localizer 3 miles out and at the proper airspeed. The pilot was instructed to continue the approach, if possible, but was given abort capability if desired (gear, flap, and engine control).

Hazard Evaluation

For each vortex encounter, the pilot was asked to make a subjective assessment of the hazard based only on the possibility of damage to the aircraft. Passenger comfort was not considered to be a factor. To assist in this assessment, rating scales and questionnaires were developed. This subjective assessment provided the only evaluation of the hazard posed by the encounter.

Table 3 Cockpit controls

Control
Column and wheel
Pitch and roll trim (thumb switch)
Rudder pedals
Throttle levers
Flap handle
Gear handle
Yaw damper ON/OFF switch

Test Conditions

The magnitude of the upset due to a vortex encounter was modulated either by varying the vortex strength or the encounter angle for encounter altitudes from 100 ft (30.5 m) to 500 ft (152.4 m). Encounters were made for two turbulence levels into either the right or left vortex, with encounter altitude and angle being selected randomly. During the preliminary phases of the program, the vortex strength was also selected randomly. However, as the test progressed and a boundary between hazardous and nonhazardous encounters became apparent, it was possible to modulate the vortex strength to give the desired encounters. Occasionally, an approach would be made without an encounter. This procedure precluded the pilot predicting when an encounter might occur, how severe it would be, and its precise nature.

Results and Discussion

Two simulator investigations were conducted to establish wake vortex encounter hazard boundaries for two widely different classes of jet transport aircraft. The first investigation was used to determine whether wake vortex encounters could be simulated with sufficient realism to permit pilot assessment of the hazard, and to define criteria (in terms of aircraft response) that provided the best correlation with pilot opinion.[10] The second investigation established hazard boundaries for the two aircraft of interest.[11]

Simulator Evaluation

Validation of the simulated wake vortex encounters was based on the subjective assessment of four pilots who had experience in intentionally encountering vortices from a B-727 and larger aircraft with a Learjet, and who also had extensive simulator experience. The task given the pilots was to fly the simulated Learjet into a wake characteristic of a B-727 and to evaluate the fidelity and realism of the encounters.

In general, the evaluation was favorable. The pilots considered the simulation and vortex encounters to be quite realistic and a good representation. In particular, they commented on the degree to which the encounter came as a surprise, even though it was highly probable that the event would occur during each simulated approach.

Adverse comments about the simulation were minor, and dealt mainly with pitch and yaw motions and accelerations that were somewhat smaller than those experienced in flight. The primary motion, that about the roll axis, was felt to be quite good. Some of the more abrupt or extreme encounters exceeded the simulator limits in terms of either rate or travel. After analyzing these data, it was found that most of these encounters fell well into the hazardous regime, and therefore did not contribute to the definition of the hazard boundary.

The turbulence model was considered to be quite good, although it was felt that the high level of turbulence, in real life, probably would have dissipated the vortices and made the encounter unlikely.

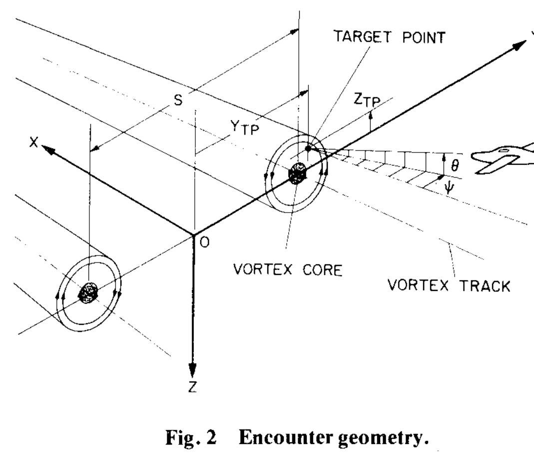

Fig. 2 Encounter geometry.

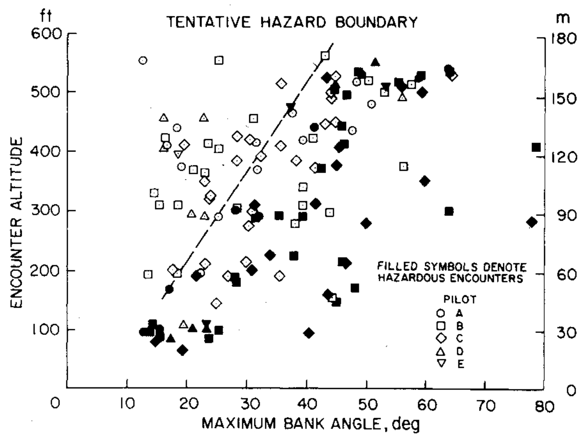

Fig. 3 Variation of encounter hazard with maximum bank angle and encounter altitude for all entry conditions, VFR.

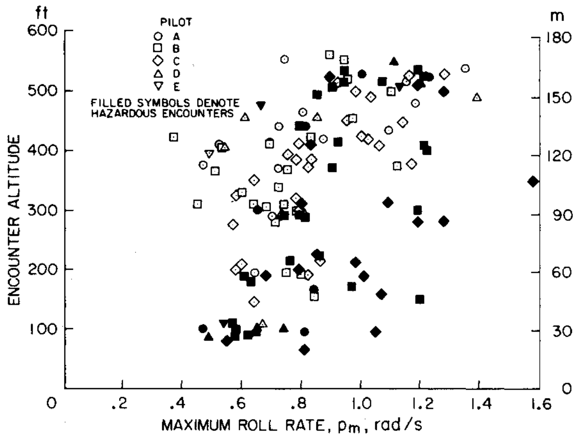

Fig. 4 Variation of encounter hazard with maximum roll rate and encounter altitude for all entry conditions, VFR.

It was concluded that the simulation provided a useful and valid method of studying piloted vortex encounters for the purposes of establishing hazard criteria.

Hazard Criteria Definition

Each pilot, on completion of a run, was asked to make a subjective assessment as to the hazard of the encounter. He was asked to rate each encounter as either hazardous or nonhazardous. Since all encounters were rated one way or the other, a boundary was sought in terms of aircraft response parameters which would segregate the data into hazardous and nonhazardous regions. Of the various parameters considered, the roll responses were thought most likely to provide the desired criterion based on observations of the relative magnitude of the responses and the fact that roll acceleration was used as a correlating parameter in data analysis from flight tests conducted at NASA's Dryden Flight Research Center.[7,14,15] Correlation on the basis of the maximum vortex-induced roll acceleration is attractive because it has the added advantage that, because this acceleration occurs prior to any pilot input, there would be no necessity for manned simulation or pilot models. In the present analysis, however, the parameter that yielded the best defined hazard boundary was maximum bank angle. This was chosen to be the maximum bank angle that occurred in response to the vortex and included any corrective action taken by the pilot to regain control. The correlation of the bank angle data from the first investigation is shown in Fig. 3 for VFR conditions. Those encounters assessed as hazardous by the pilots are designated by the filled symbols. The hazard boundary shown clearly separates the data into two regions: one containing no hazardous encounters, and one in which the encounter is likely to be hazardous.

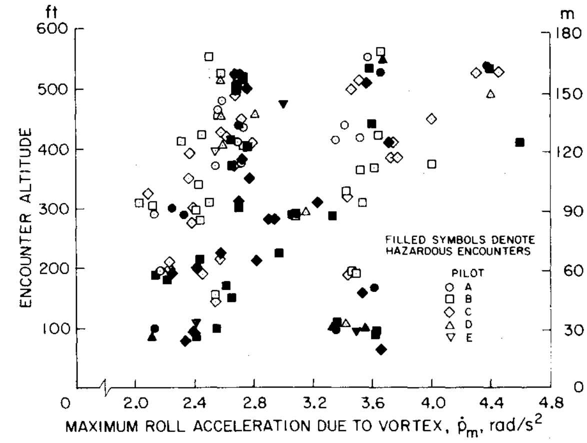

Fig. 5 Variation of encounter hazard with maximum roll acceleration due to the vortex and encounter altitude for all entry conditions, VFR.

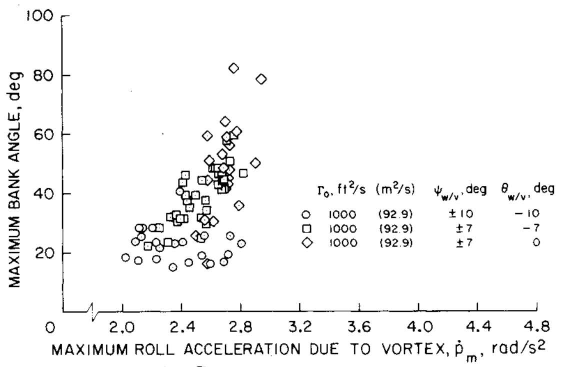

a) Constant vortex strength

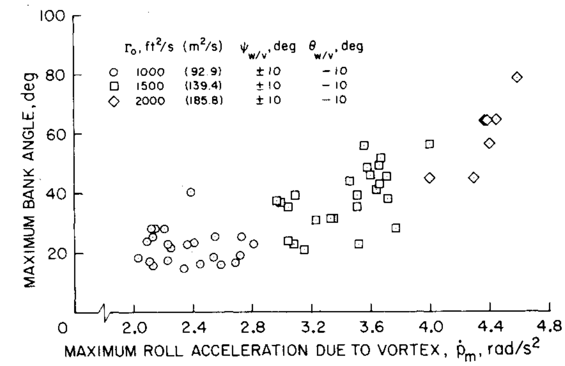

b) Constant encounter angle

Fig. 6 Variation of the maximum bank angle with the maximum roll acceleration due to the vortex.

Correlation of the pilots' assessment of hazard with either roll rate or roll acceleration was considerably less successful. The correlation of the data in terms of maximum roll rate is shown in Fig. 4. Although some separation of the data into hazardous and possibly hazardous regions is evident, a boundary cannot be drawn that separates as many of the nonhazardous encounters from the data set as was possible in the case of maximum bank angle.

The correlation of the pilots' assessment of hazard with maximum roll acceleration is shown in Fig. 5. These results are of particular interest since, as previously mentioned, roll acceleration has been used as a correlation parameter for analyzing flight data. The parameter used in the flight program was the ratio of the vortex-induced roll acceleration to the roll control power of the airplane. Since, for a given flight condition, the roll control power of the aircraft is a constant, this parameter is analogous to that used in Fig. 5. In terms of this parameter, the nonhazardous encounters were found to be randomly distributed throughout the range of the data (Fig. 5), and definition of a hazard boundary that separates a significant number of nonhazardous encounters from the rest of the data is not possible.

Since, for these tests, the severity of the encounter was controlled by varying either the vortex strength or the encounter angle independently, the magnitude of the upsets (bank angles) could be varied by a similar amount for either case. However, as shown in Fig. 6, only when the encounter angle was held constant did the maximum bank angle show any significant variation with the vortex-induced roll acceleration. Since it has been shown already that bank angle correlates the hazard assessment (Fig. 3), it follows that this restricted data set (constant encounter angle) also should correlate the data. Such a correlation is shown in Fig. 7.

It is speculated that flight test procedures[7,14,15] limited the encounter angles to a much smaller range than those covered in the simulation. If this range was sufficiently small, the simulation results demonstrate that an assessment of hazard in terms of maximum roll acceleration due to the vortex should provide a correlation of the data.

Hazard Boundaries

Comparison of Simulators

A comparison of the hazard assessment in terms of maximum bank angle from the two investigations is shown in Fig. 8. These results are restricted to three pilots who flew both simulations and, in addition, were responsible for the majority of the data obtained during the first simulation. On the basis of these data, a more conservative hazard boundary would be drawn from the FSAA data than for the 6-DOF data. However, this boundary would encompass only four hazardous encounters that lie outside the 6-DOF boundary.

It was noted from Fig. 3 that, for these preliminary results, the boundary appeared to be representative of the opinion of all of the participating pilots, in that each rated hazardous at least one encounter that lay near the boundary. The data presented in Figs. 9-12, however, indicate that this unanimity did not exist during the second investigation. For instance, the results for VFR approaches for the Learjet (Fig. 9) indicate a boundary more conservative than would be drawn on the basis of the data shown in Fig. 8. The difference in the two boundaries is the result of two encounters rated as hazardous by pilot E at nominal altitudes of 350 and 500 ft. Similar situations are evident in other results for both VFR and IFR conditions.

It should be pointed out that the mathematical representation of the Learjet was somewhat different for the two simulations as a result of the different emphasis placed on each experiment. Since the emphasis during the first simulation was placed on establishing that the simulated encounters were comparable to those experienced by the pilots in flight, a similar aircraft model was required. This model thus specified that the yaw damper be engaged at all times. However, the emphasis during the second simulation was to establish boundaries for the landing approach task. Standard operating procedure for landing approach requires the yaw damper to be disengaged during the approach. Thus, the math models used for the second simulation for both airplanes specified that the yaw damper be disengaged at all times.

Hazard Boundaries for Learjet and Boeing 707/720 Aircraft

Hazard boundaries have been drawn in Figs. 9-12 for altitudes from 50 to 500 ft for VFR conditions and from 200

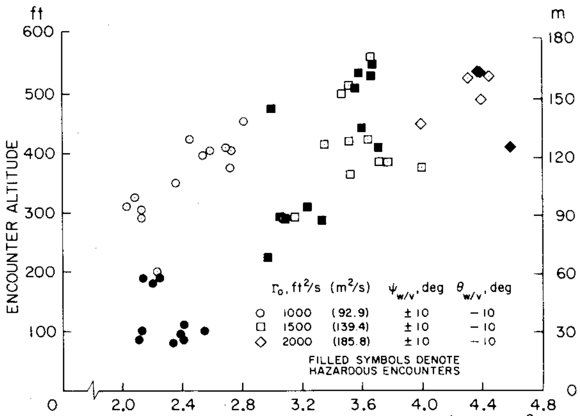

Fig. 7 Variation of encounter hazard with encounter altitude and maximum roll acceleration due to the vortex, VFR.

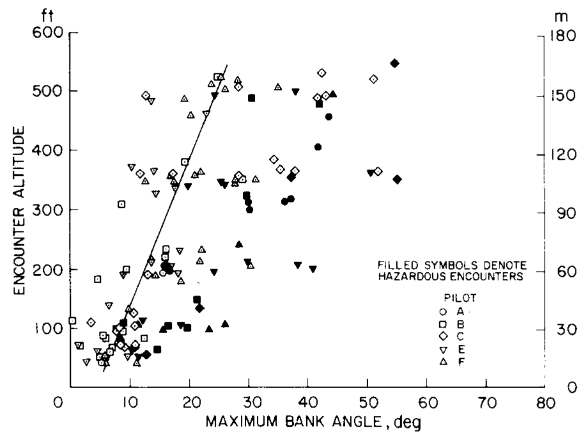

Fig. 9 Variation of encounter hazard with maximum bank angle and encounter altitude, Learjet/VFR.

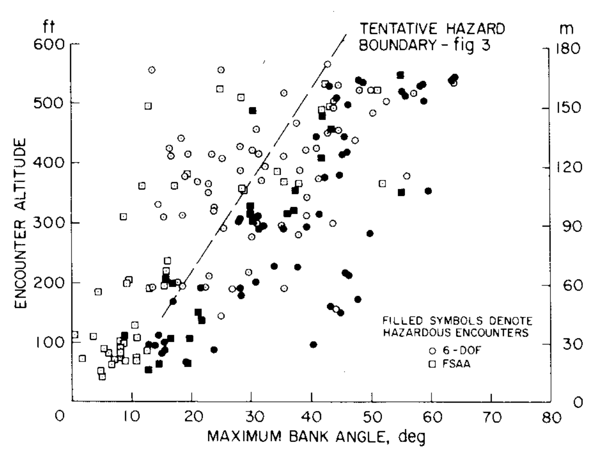

Fig. 8 Comparison of hazard boundary for two simulators, Learjet/VFR.

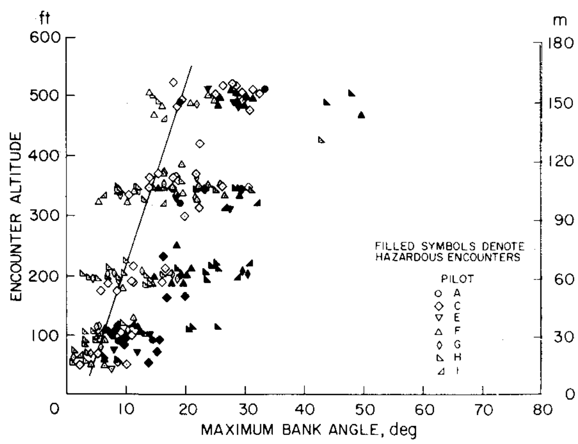

Fig. 10 Variation of encounter hazard with maximum bank angle and encounter altitude, Boeing 707/720/VFR.

to 500 ft for IFR conditions for both the Learjet Model 23 and the Boeing 707/720 from the second investigation. These boundaries separate the data into two regions; one containing only nonhazardous encounters, and the other containing both hazardous and nonhazardous encounters. Thus, these boundaries, as drawn, represent the most conservative rating of all of the pilots, even though it has been shown previously that the boundaries drawn for individual pilots vary considerably. It also can be seen from these data that the band of nonhazardous encounters included in the potentially hazardous region is more widespread at the higher altitudes than at the lower altitudes. Thus, in essence, this can be considered to be scatter in the data which reflects the latitude available to the pilot in making his subjective assessment of the hazard. A decrease in the amount of scatter thus represents a more conclusive assessment of the hazard.

For VFR flight conditions, both the maximum acceptable bank angle and the scatter in the data decreased markedly with decreasing altitude. For example, at an altitude of 100 ft, the boundaries shown in Figs. 9 and 10 show maximum acceptable bank angles of 6-8° and a scatter of about 6°. At an altitude of 500 ft, however, the maximum acceptable bank angles increase to 20-25°, depending on aircraft type, with the amount of scatter increasing to 25-30°.

For IFR flight conditions (Figs. 11 and 12), the maximum acceptable bank angle remains constant at altitudes above 350 ft, but decreases significantly at the lower altitudes. The scatter in the data is comparable to that obtained under VFR conditions for comparable altitudes.

The hazard boundaries shown in Figs. 9-12 are summarized in Fig. 13 for both the Learjet and the Boeing 707/720, for both VFR and IFR flight conditions. For VFR conditions, the

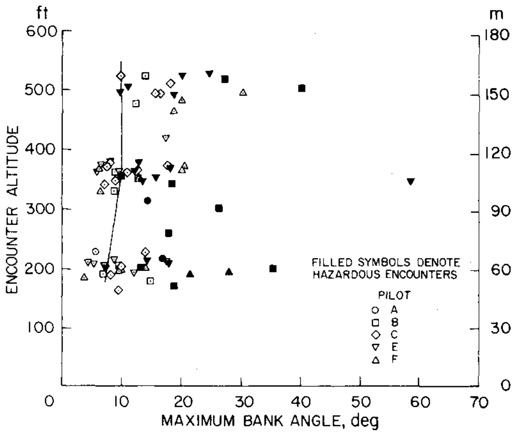

Fig. 11 Variation of encounter hazard with maximum bank angle and encounter altitude, Learjet/IFR.

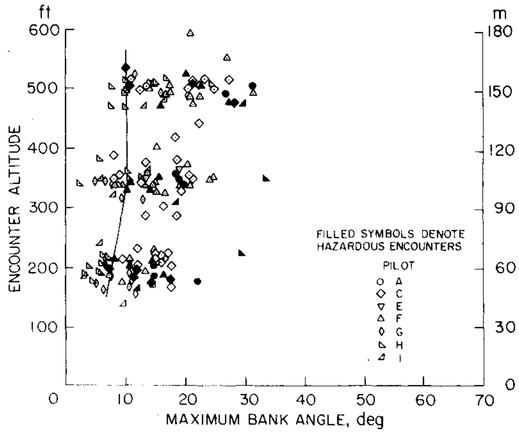

Fig. 12 Variation of encounter hazard with maximum bank angle and encounter altitude, Boeing 707/720/IFR.

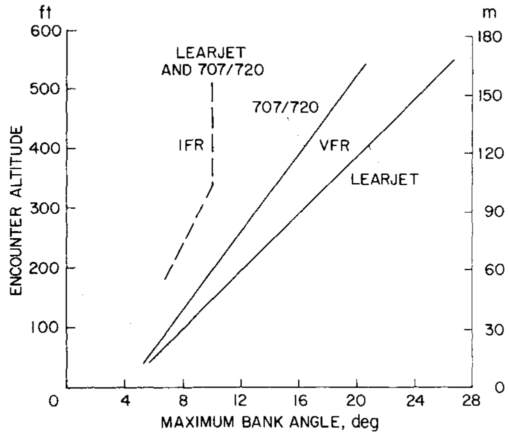

Fig. 13 Indicated hazard criteria for Learjet and Boeing 707/720 for both VFR and IFR flight conditions.

hazard boundary is nearly the same for both aircraft at the lower altitude, but diverges with increasing altitude. As might be expected, the hazard boundary for the larger aircraft is the more conservative. As noted previously, the hazard boundary under IFR conditions for both aircraft remained constant at about 10° for altitudes above 350 ft, but decreased to about 7° at the breakout altitude of 200 ft. The hazard boundary for IFR conditions is shown to be on the order of 50% of that for VFR conditions for the larger aircraft. For both VFR and IFR conditions, upsets as small as 7° in bank angle were considered hazardous at the lower altitudes.

Pilot Comments

Comments by the pilots in response to specific questions were analyzed to reveal any consistent patterns that could be used to augment the results presented previously. The following items were indicated:

1) In general, the upsets were felt to be quite realistic, particularly with regard to roll response.

2) In most cases, the encounters were easily distinguishable as being vortex generated in either smooth air or moderate turbulence. This is of particular interest for the smaller upsets because the question arises as to whether a vortex encounter can be distinguished from upsets due to normal atmospheric turbulence. It was determined from responses to the pilot questionnaire that, for maximum bank angles of 5-10° due to the vortex, 88% of the encounters in smooth air were recognized as being vortex generated. When moderate turbulence was present, the ability of the pilots to differentiate between upset type was reduced to 69%.

3) The primary reason for rating an encounter as hazardous was proximity to the ground at the time of the encounter or subsequent altitude loss as a result of the encounter. This is reflected in the reduction in the maximum bank angle at the hazard boundary and in the more consistent ratings as altitude is decreased.

4) Misalignment with the runway and/or glideslope was frequently cited as the reason for a hazardous rating because of the dangers involved in attempting to recover and reacquire the track. Misalignment on the approach generally resulted from an encounter that tossed the aircraft to one side or below the glideslope.

5) Disorientation associated with encounters under instrument conditions and sudden or violent upsets that startled the pilots were additional factors leading to hazardous ratings.

Concluding Remarks

Piloted six-degree-of-freedom motion simulator investigations conducted at the NASA Ames Research Center demonstrated that wake vortex encounters could be reproduced realistically on a simulator, and that maximum bank angle due to the encounter best correlates the pilots' subjective assessment of the hazard.

Boundaries separating nonhazardous and potentially hazardous wake vortex encounters during a landing approach task have been obtained for a light twin-jet (Learjet) and for a four-jet transport (Boeing 707/720) for both VFR and IFR flight conditions. For VFR conditions, boundaries for both are the same at the lower altitudes, becoming more conservative for the larger aircraft. For IFR conditions, boundaries are the same for either aircraft and about 50% less than those for VFR conditions. Upsets as small as 7° in bank angle were considered hazardous at the lower altitudes for both flight conditions. Proximity to the ground was the primary reason for a hazardous rating, and the pilots' consistency in ratings increased significantly as the altitude decreased.

References

[1] Israel, D. R., "Air Traffic Control: Upgrading the Third Generation," *Technology Review*, Vol. 77, March 1975, pp. 14-24.

[2] Roberts, L., "On Wake Vortex Alleviation," presented at NASA/University Conference on Aeronautics, University of Kansas, Oct. 23-24, 1974.

[3] Anon., FAA Symposium on Turbulence, Washington, D. C., March 22-24, 1971.

[4] McCormack, B. W., "Aircraft Wakes: A Survey of the Problem," presented at FAA Symposium on Turbulence, Washington, D. C., March 22-24, 1971.

[5] Kirkman, K. L., Brown, C., and Goodman, A., "Evaluation of Effectiveness of Various Devices for Attenuation of Trailing Vortices Based on Model Tests in a Large Towing Basin," NASA CR-2202, 1973.

[6] Garodz, L. J., Hanley, W. J., and Miller, N. J., "Abbreviated Investigation of the Douglas DC-10 Airplane Vortex Wake Characteristics in Terminal Area Type Operations," FAA/NAFEC Project No. 214-741, 04X (Special Task NoYF FS-2-73), Federal Aviation Administration (FAA), National Aviation Facilities Experiment Center (NAFEC), Aug. 1972.

[7] Barber, M. R., Kurkowski, R. L., Garodz, L. J., et al., "Flight Test Investigation of the Vortex Wake Characteristics Behind a Boeing 727 During Two-Segment and Normal ILS Approaches," NASA TM X-62, 398, 1975 (NA-75-151, 1975, FAA).

[8] Elson, B. M., "Reduction in Aircraft Separations Sought," *Aviation Week and Space Technology*, Vol. 103, July 28, 1975, pp. 48-51.

[9] Johnson, W. A. and Meyers, T. T., "A Model for Human Pilot Behavior During Wake Vortex Encounter Upsets," Systems Technology, Inc., Hawthorne, Calif., TR-1035-5, 1976, (FAA RD-76-8, 1976).

[10] Sammonds, R. I. and Stinnett, G. W., Jr., "Hazard Criteria for Wake Vortex Encounters," NASA TM X-62, 473, 1975.

[11] Sammonds, R. I., Stinnett, G. W., Jr., and Larsen, W. E., "Wake Vortex Encounter Hazard Criteria for Two Aircraft Classes," NASA TM X-73,113, 1976, (FAA RD-75-206, 1976).

[12] Jewell, W. F. and Stapleford, R. L., "Mathematical Models Used to Simulate Aircraft Encounters with Wake Vortices," Systems Technology, Inc., Hawthorne, Calif., TR-1035-4, 1975 (FAA DOT-FA73WA-3276-1, 1975).

[13] Johnson, W. A. and Rediess, H. A., "Study of Control System Effectiveness in Alleviating Vortex Wake Upsets," AIAA Paper 73-833, Key Biscayne, Fla., 1973.

[14] Andrews, W. J., Robinson, G. H., and Larson, R. R., "Exploratory Flight Investigation of Aircraft Response to the Wing Vortex Wake Generated by Jet Transport Aircraft," NASA TN D-6655, 1972.

[15] Robinson, G. H. and Larson, R. R., " A Flight Evaluation of Methods for Predicting Vortex Wake Effects on Trailing Aircraft," NASA TN D-6904, 1972.